

Solute Transport in Sediments by a Large Freshwater Oligochaete, *Branchiura sowerbyi*

XIAOSONG WANG[†] AND
GERALD MATISOFF*

Department of Geological Sciences, Case Western Reserve
University, Cleveland, Ohio 44106

Laboratory experiments using the radionuclide ^{22}Na as a solute tracer were conducted in microcosms containing the freshwater tubificid oligochaete, *Branchiura sowerbyi*, to determine the exchange of solutes between sediments and overlying water. Three different mathematical models of solute transport in sediments are applied to the data to evaluate which modeled processes best quantifies solute exchange by *B. sowerbyi* and how that exchange is affected by worm density. An enhanced diffusion model, in which the solute diffusion coefficient is higher in the bioturbated zone than in unmixed sediments best described the data. At population densities of 4000 and 8000/m², the effective diffusivity of ^{22}Na , D_e , is 1.87 and 4.78 times that in the absence of the worms, respectively (91.69 and 234.9 cm²/yr as compared to 49.17 cm²/yr in the control). A cylindrical burrow model does not describe the transport processes well, presumably because *B. sowerbyi* does not actively irrigate its burrows and abandoned burrows do not remain open for fluid exchange with the overlying water. A nonlocal exchange model with a constant exchange coefficient within the mixing layer also was found to be inadequate to describe solute transport. A depth-dependent exchange coefficient might yield better agreement with the data but would still be inferior to the enhanced diffusion model. The nonlocal exchange model and the cylindrical burrow model yield similar results as predicted by Boudreau (*J. Mar. Res.* **1984**, 42, 731–735).

Introduction

Nearly all recent fine-grained sediment deposits are inhabited by infaunal macroinvertebrates. These animals through their burrowing, feeding, excretion, respiration, and locomotion activities not only cause particle mixing but also cause fluid transport across the sediment–water interface. Such biogenically induced transport has major direct and indirect effects on the composition of sediments and their overlying waters and on the recycling of buried materials. Burrows act as channels for the direct communication between interstitial and overlying waters; fecal pellets deposited on the sediment surface increase the porosity of the uppermost sediment and therefore increase the diffusional exchange; and the injection of surface water for burrowing and feeding modifies the porosity and chemical conditions in the sediment and increases the exchange of water and solutes across the sediment–water interface.

* Author to whom correspondence should be addressed; telephone: (216)368-3677; fax: (216)368-3691; e-mail: gxm4@po.cwru.edu.

[†] Present address: South Florida Water Management District, Department of Regulation, 3301 Gun Club Road, West Palm Beach, FL 33406.

Some benthos (bioirrigators) construct permanent or semi-permanent burrows and pump overlying water through them (2–4). Other benthos [conveyor-belt feeders (5)] feed head first in the sediment and deposit fecal pellets onto the sediment surface. The mixing of sediment particles by conveyor-belt feeders has been well studied (6, 7). However, studies of solute transport by conveyor-belt feeders is limited (8, 9). Although McCall and Fisher (8) reported that the presence of a pelletal layer by *Tubifex tubifex* enhanced diffusive transport, Krezoski *et al.* (9) found that the dispersion coefficient in reworked sediments with *Stylodrilus* killed was approximately the same as that in the control cells. These results suggest that active particle reworking may actually be responsible for the observed enhanced solute transport. Because conveyor-belt deposit feeding oligochaetes are abundant in recent freshwater sediments but their effect on solute exchange between sediments and water is not well known, this study was conducted to evaluate the role of a large deposit feeding oligochaete on solute transport. Here, we present experimental results for the large freshwater tubificid oligochaete *Branchiura sowerbyi*. The exchange of solutes between sediments and overlying water was studied using a radionuclide tracer, ^{22}Na , in laboratory microcosms with different densities of *B. sowerbyi*. Three different mathematical models of solute transport in sediments will be applied to the data to evaluate which modeled process best quantifies solute exchange by *B. sowerbyi* and how that exchange is affected by worm density.

Branchiura sowerbyi is a head down deposit feeding tubificid oligochaete (10). *B. sowerbyi* has a deep red color, and the adult is usually about 10 cm long, although in this study some worms were observed to extend to 15 cm. The population density of *B. sowerbyi* was not measured at the time of collection, but Kikuchi and Kurihara (10) reported a population density of 8842 individuals/m². *B. sowerbyi* in ricefield soils in Japan, and Soster (11) reports *B. sowerbyi* abundances has high as 584 individuals/m² for the western basin of Lake Erie.

B. sowerbyi worms are very efficient burrowers. Normally the adults build vertical and cross-connected burrows in the substratum extending from below the sediment–water interface to a depth of over 20 cm. They stay in the burrows only for a short period of time and then move to a new location to build new burrows. The abandoned burrows are usually destroyed or sometimes become a part of the newly built burrows. Inside the burrows, the worms selectively ingest silt and clay particles, feed on attached microflora, mix the injected sediments in their guts, and expel the feces onto the sediment surface as cylindrical, mucus-bound, fecal pellets (9, 12). They also wave their posterior region in the overlying water and irrigate the sediment with their burrows.

Kikuchi and Kurihara (10) found that the presence of *B. sowerbyi* worms kept the activity of Fe²⁺ high in the upper 1 cm of the sediment, increased the flux of Fe²⁺ into the overlying water, enhanced ammonia concentration in the sediment, decreased the number of aerobic bacteria, and increased the number of sulfate-reducing bacteria throughout the sediment column. The experiments in this study also showed that *B. sowerbyi* transports large quantities of sediment particles from deeper reduced zones onto the sediment surface during burrowing and feeding, creating a surficial zone of fecal pellets and high porosity sediment about 5 cm thick.

Methods

Sediments and living macrofauna were collected from the profundal zone of the western basin of Lake Erie during June

1993 using a PONAR grab sampler. Bottom sediments at the sampling sites were composed mainly of silt and clay; water depths were about 10 m, and water temperatures were about 12 °C. Sediments and living macrofauna were placed in a 40-L bucket and covered with Lake Erie water. The samples were then transported to the laboratory at Case Western Reserve University, Cleveland, OH, within 4 h.

Upon arrival in the laboratory, the sediment was prepared for use in the microcosms in the following manner. Small sediment samples were forced through a 500- μ m mesh sieve by applying hand pressure. This process removes coarse sand particles and debris from the sediment and also kills the majority of the macrobenthos. After sieving, the sediment samples were held overnight in a refrigerator at 5 °C. Then the sediment samples were maintained in a bucket with Lake Erie water at room temperature (20 °C) to prevent them from drying.

Live worms were obtained by gently rinsing small quantities of the collected sediment through a 1-mm mesh sieve with tap water. The worms retained in the sieve were carefully transferred into small plastic boxes (10 \times 10 \times 12 cm i.d.) that contained Lake Erie mud and water. These boxes were then transferred into a 40-L well-aerated aquarium and maintained at 12 °C. The animals were usually maintained in the laboratory for about 2–10 days before they were used. In this study, all the animals were alive and active when they were used in the experiments.

The ^{22}Na tracer was purchased in the form of carrier-free NaCl aqueous solution, which was in a form suitable for solute tracing experiments. Sodium is in dissolved form and is considered a conservative ion in lake water. It is adsorbed only weakly by certain types of sediment particles. Krezoski *et al.* (9) measured the distribution coefficient of ^{22}Na in microcosm sediments collected from southern Lake Michigan and obtained a value of 0.17. Thus, ^{22}Na is a good tracer of solute transport. The half-life of ^{22}Na is 2.2 yr, which is also long relative to the experimental duration so that radioactive decay of ^{22}Na during the course of an experiment is insignificant.

The experimental microcosms were made of rectangular plastic cells 5 \times 1 \times 30 cm i.d. (Figure 1). The preparation of experimental microcosms includes three major steps: (1) loading sediments, (2) adding radioactive tracers, and (3) loading experimental animals. Previously prepared Lake Erie sediments were first drawn into a syringe and then slowly injected into each cell through Tygon tubing until a 20–25 cm sediment column was built. Several thin layers containing ^{137}Cs -labeled clay were incorporated into the sediment column to trace particle mixing (reported elsewhere). After the sediments were loaded into cells, 6–10 cm overlying water was added to each cell. The cells were placed into a 40-L aquarium and the sediments were allowed to compact for 5–10 days at 12 °C. Each cell was elevated so that the top edge was about 1 cm above the aquarium water level. The overlying water column in every cell was aerated with one or two aquarium air bubblers connected with Tygon tubing. After the rate of sediment compaction slowed (determined by monitoring the downward migration of the sediment–water interface), worms were measured and then transferred into the cells. The control cell received no worms while 2 *B. sowerbyi* worms (~ 4000 individuals/ m^2) or 4 *B. sowerbyi* worms (~ 8000 individuals/ m^2) were added to the treatment cells. Worms were allowed to acclimate in the new environment for several hours and were usually active and burrowed into the sediment very quickly. The cells were loosely covered with a plastic cap to prevent splattering of radioactive overlying water by air bubbles.

About 3×10^6 Bq ^{22}Na was added to a 2-L water reservoir that was connected to the experimental system with Tygon tubing through a peristaltic pump. The activity of ^{22}Na in the overlying water of each cell was kept constant during the

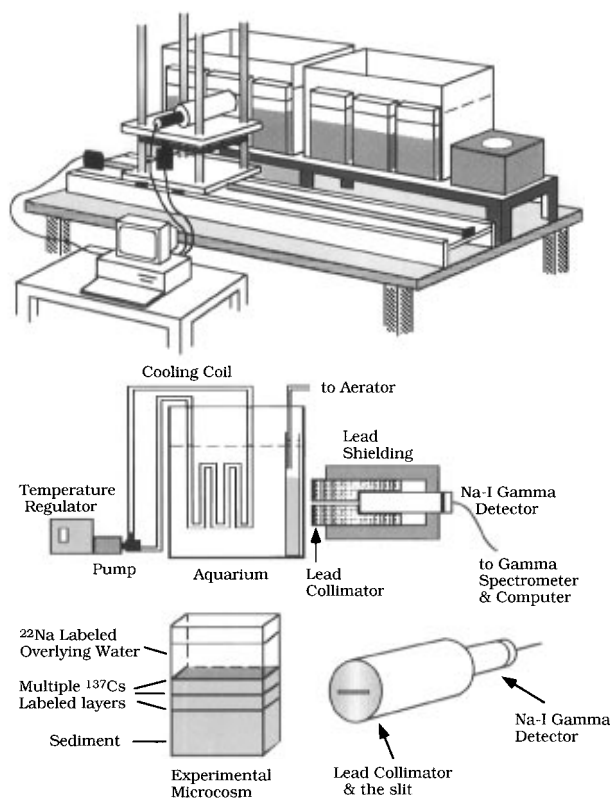


FIGURE 1. Experimental γ -scan system. The top illustration shows the general layout of the equipment, the middle illustration shows a side view of the collimator/detector, and the bottom figure illustrates the solute tracer in a microcosm and the slit in the collimator.

entire experiment by using the peristaltic pump to circulate the overlying water through the reservoir. The total overlying water volume of 3–4 cells consists of only 4–5% of the total volume of water in the reservoir.

The γ -scanner system includes a 2 in. \times 2 in. NaI γ -detector coupled to a multi-channel analyzer and a computer-controlled positioning system (Figure 1). The NaI detector is well shielded from all incident radiation except from a collimated slit (0.4 cm \times 5 cm) extending the full width (5 cm) of an experimental cell. The shielding consists of a solid lead cylinder 13 cm thick in front and 2.5 cm thick on the side. Because of the high background contributed by the ^{22}Na 1.275 MeV γ -ray, an extra 5 cm thick lead shielding was built around the detector using lead bricks. The whole detector is placed on an aluminum plate connected to an X-Y slider by four vertical screw rods. Smooth horizontal and vertical movement and precise positioning are automatically controlled by two computer-operated stepper motors. The accuracy in repositioning the detector is within 0.01 mm.

Tracer activity profiles were obtained by vertically scanning the outside wall of each cell at 2–2.5 mm intervals for 6 min. Tracer activities at each depth interval were automatically recorded and stored on the computer along with scan positions and scan time periods. A single scan of a cell took about 1.5–2 h. Because the sediment inside each cell was not disturbed during the scanning process, time series migrations of tracer nuclides were monitored by periodically scanning each cell. The background ^{22}Na activity was subtracted from each scan profile. The sediment–water interface was gradually moving down during the experiment due to sediment compaction. The interface in both cells containing *B. sowerbyi* moved down ~ 0.8 cm. In the control cell, it moved down ~ 0.2 cm. This effect was corrected in the scan profiles by recording the actual interface position at the start of each scan.

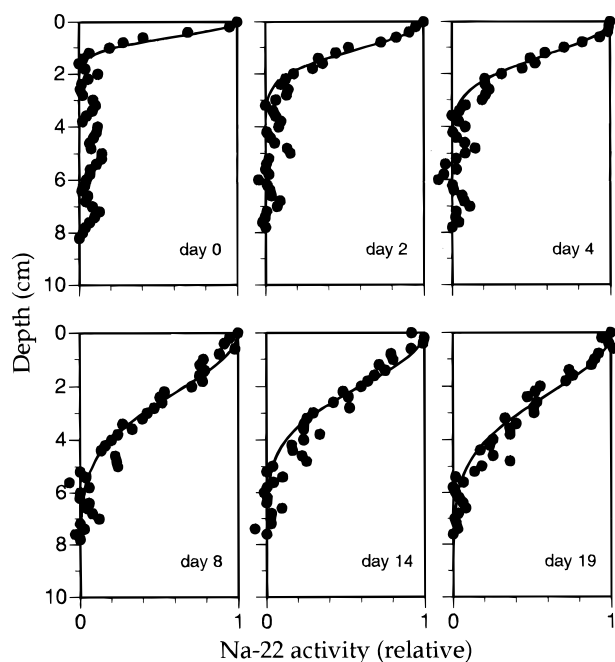


FIGURE 2. ^{22}Na activities in the sediments in the control cell over a 19-day time period. Solid circles are measured activities. Lines are least squares Gaussian fits used to determine D_e . Data are background corrected and normalized relative to the activity at the sediment–water interface.

We observed that organisms usually mixed sediment more intensely during the first few days of an experiment and that ^{22}Na diffusion across the sediment–water interface was much faster during the initial stage of an experiment because of the sharp concentration difference between the overlying water and the pore fluid. Therefore, the cells were scanned on a daily basis during the first week of the experiment and then twice a week after that. The experiment continued for 31 days.

After the experiments were completed, the porosity was measured using a ^{109}Cd γ -ray adsorption technique (13) based on the fact that the weak 0.088 MeV emission from the ^{109}Cd nuclide is partially attenuated when it penetrates through a sediment column. If the thickness of the sediment column and the detector geometry are fixed, then the attenuation of the ^{109}Cd γ -emission will be different for sediment having different porosities. The control cell and the cell with 2 *B. sowerbyi* had porosities equal to 0.8 and the cell with 4 *B. sowerbyi* had a porosity equal to 0.67. In all three cases the porosities were nearly vertically homogeneous.

Results

The scanned ^{22}Na activity profiles for the three experimental cells are shown in Figures 2–4. The vertical axis is the depth from the sediment–water interface. The horizontal axis represents the activity of ^{22}Na in the sediment relative to the activity at the sediment–water interface (overlying water concentration). Only the data in the first 19 days are shown, because the activity of ^{22}Na after the 19th day approached a uniform value throughout the cells. Figure 2 shows the transport of ^{22}Na across the sediment–water interface in the control cell. Since there were no organisms in this cell, transport was entirely due to ionic diffusion. It can be seen that ^{22}Na diffusion is fairly rapid in sediments of high porosities ($\sim 80\%$) such as Lake Erie mud. The 50% concentration front moved down ~ 2 cm from a depth of 0.5 cm to 2.5 cm within 14 days. After that the diffusion was less due to a smaller concentration gradient as the transport profile approached steady state. Figure 3 shows the transport of ^{22}Na in the cell with 2 *B. sowerbyi* worms. The transport profiles in this cell

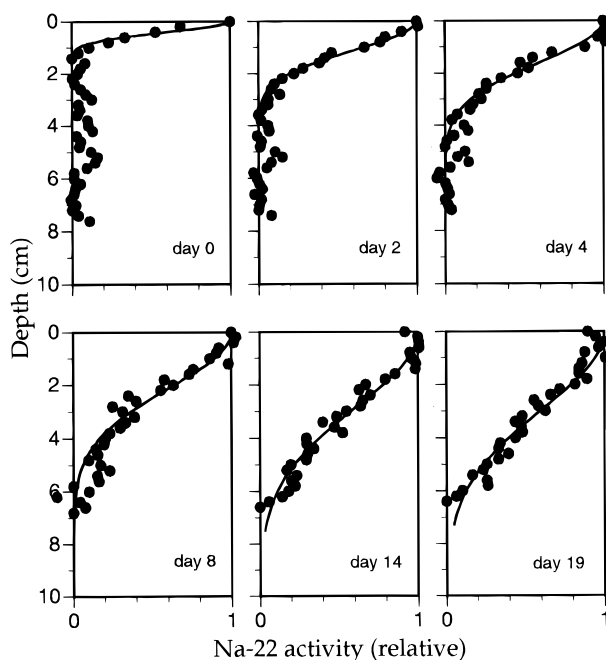


FIGURE 3. ^{22}Na activities in the sediments in the cell with 2 *B. sowerbyi* worms (~ 4000 individuals/ m^2) over a 19-day time period. Solid circles are measured activities. Lines are least squares Gaussian fits used to determine D_e . Data are background corrected and normalized relative to the activity at the sediment–water interface.

also show some similarities to those obtained from the control cell in that they look like an ionic or Fickian diffusional transport with the maximum concentration at the sediment–water interface. However, comparison of the scan profiles from the two cells indicates that the 50% concentration front moved down farther in the cell with the worms [3.0 cm (from 0.5–3.5 cm) within 14 days] than in the control cell. This indicates that the diffusion of ^{22}Na was somehow enhanced by the organisms. The ^{22}Na transport profiles from the cell with 4 *B. sowerbyi* worms are shown in Figure 4. With an increased population density, the transport rate was even higher. After 14 days, the 50% concentration front had moved down 5 cm in this cell (from <1 to 5 cm). After 19 days, the profile was approaching a uniform shape. We observed during the experiment that the worms burrowed to a depth of ~ 10 cm (equivalent to their body length) immediately after being placed in the microcosm and deepened their burrows to a depth of 17–20 cm within several days. Sediments were vertically transported by conveyor-belt feeding, forming a mixed pelletal layer ~ 5 cm thick. At the same time, the worms were moving up and down in the burrows transporting particles vertically from depth to the surface. The pelletal layer and the burrows might have decreased sediment tortuosity and, thus, the rate of solute transport. The higher transport rate of ^{22}Na at higher population densities is likely the result of more burrowing activity at the higher population density.

Solute Transport Models

Several different transport models have been proposed to simulate solute transport in sediments inhabited by macrobenthos. These models can be categorized into four major classes. Enhanced vertical diffusion models assume a multiple-layered sediment in which macrofaunal effects on solute exchange can be accounted for in a single increased effective or apparent diffusion coefficient within the bioturbated zone (8, 14–21). These models are good for situations in which the biological mixing in sediment is intense and does not involve strong advective flow of fluid in any direction. The second class is termed advection or biopumping models

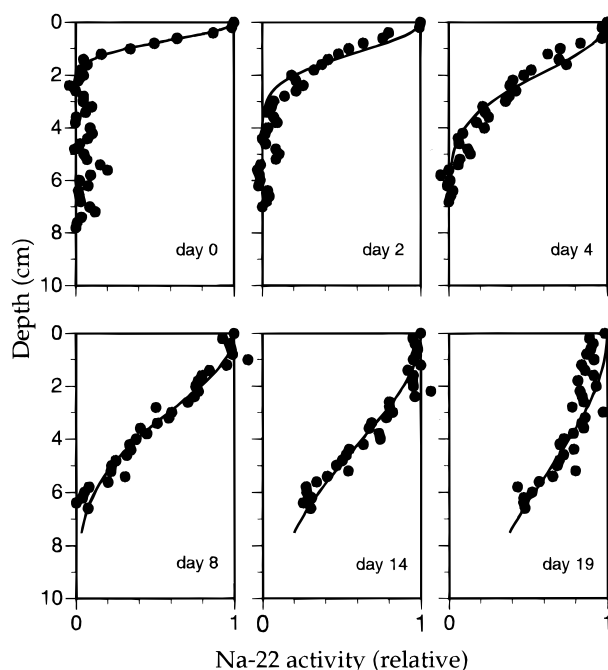


FIGURE 4. ^{22}Na activities in the sediments in the cell with 4 *B. sowerbyi* worms (~ 8000 individuals/ m^2) over a 19-day time period. Solid circles are measured activities. Lines are least squares Gaussian fits used to determine D_e . Data are background corrected and normalized relative to the activity at the sediment–water interface.

(22). These models assume that pore water is biologically advected or pumped between discrete well-mixed layers in the sediment and the overlying water. Such biopumping processes normally occur when organisms construct permanent or semi-permanent burrows and irrigate them with the overlying water or when the mixing rate is high so that solutes which enter the sediment are quickly mixed throughout the bioturbated zone. An exchange or biopumping rate constant is a characteristic of this kind of model. Exchange rates calculated by advection or biopumping models can be a factor of 2 or more higher than predicted by a one-dimensional enhanced diffusion model. The third class of model was first developed by Aller (23–25) and was termed a three-dimensional diffusion model or cylindrical diffusion model (21). This type of model assumes that specific changes in the average geometry of diffusion in sediment results from the presence of irrigated burrow and tube structures and that the sediment body as a whole can be represented by an average microenvironment that is composed of a single, irrigated burrow cylinder and its surrounding sediment. This model works nicely when the sediment is dominated by sedentary, suspension-feeding vertical burrowers, such as chironomids (26). Recently, a fourth class of model has become popular. This model was used by Emerson *et al.* (27) and is defined by Imboden (28) as a nonlocal exchange model (29–38). This model is basically an approximation of Aller's cylindrical burrow model with only a single transport parameter (1), but it has the advantage that transport profiles in sediment with complicated structures can be adequately simulated by suitably defining a nonlocal exchange coefficient. This model, however, does not describe the actual transport processes occurring in the sediment.

In this study we will apply the enhanced diffusion model, the cylindrical burrow model, and the nonlocal exchange model to the data to permit evaluation and comparison of the different models. The advection or biopumping model will not be evaluated because the worms studied here do not appear to induce the stirring process described by that model. The equations are solved numerically by a finite difference

approximation, and the computer programs are presented elsewhere (13).

Enhanced Diffusion Model. The enhanced diffusion model is an extrapolation of the transient diffusion model of pore fluid in the absence of benthic organisms (39). This model assumes that all macrofaunal effects on the exchange of solute i in the mixed layer can be accounted for in a single increased effective or apparent diffusion coefficient, D_e , in the mixed layer. This D_e is actually the combined result of molecular diffusion and biodiffusion in sediment. Below the mixed layer, the molecular diffusion coefficient of species i in the bulk sediment, D_s , is the same as in the absence of mixing. Assuming that ^{22}Na is chemically conservative and does not adsorb onto sediment particles, then the model can be mathematically described as

$$\frac{\partial C_i}{\partial t} = D_e \frac{\partial^2 C_i}{\partial x^2} - \lambda C_i \quad (1)$$

where C_i is the activity of ^{22}Na in the mixed layer (decays/s); λ is the radioactive decay constant of ^{22}Na (s^{-1}); x is depth from the sediment–water interface (cm, positive down); and t is time (s). A mixed layer of thickness L and the underlying sediment are coupled by requiring that the concentrations at the boundary between the layers and the flux across the boundary be continuous. The activity of ^{22}Na at the sediment–water interface, C_0 , was kept constant during the entire experiment. At depth, the ^{22}Na activity gradient approaches zero. The mixed depth is determined from the particle mixing results (26). For the cell with 2 worms this mixing depth is 13.6 cm, and for the cell with 4 worms it is 11.7 cm.

The only parameters that need to be determined with this model are the biodiffusion coefficient, D_e , and the diffusion coefficient of ^{22}Na in the sediment, D_s . Since the model treats bioturbation as a diffusive process, D_e and D_s can be calculated from a plot of the square of the standard deviation of the concentration front broadening versus time in the control cell and the experiment cells containing organisms, respectively (13, 40).

Cylindrical Diffusion Model. Aller (19, 23–25) presented a model for solute transport in the presence of irrigated burrows. In this model the sediment is approximated as a mosaic of micro-environments, each of which is the same size and can be represented by a central irrigated vertical burrow and its nearby surrounding sediment. There are three major solute transport processes involved in this micro-environment: (1) vertical molecular diffusion across the sediment–water interface; (2) direct exchange of solutes between the overlying water and the burrow due to burrow irrigation or biogenic pumping; and (3) diffusion of solutes radially across the burrow wall. The sediment can be divided into two distinct zones of transport regimes: an upper zone extending from the sediment–water interface to the bottom of average burrows in which all the above processes are involved and a zone below the upper zone encompassing the remainder of the sediment column where vertical molecular diffusional transport dominates. Mathematically, the change of solute activity with time in the sediments in the upper, mixed zone can be described as

$$\frac{\partial C_i}{\partial t} = D_s \frac{\partial^2 C_i}{\partial x^2} + D_r \frac{\partial^2 C_i}{\partial r^2} + \frac{D_r}{r} \frac{\partial C_i}{\partial r} - \lambda C_i \quad (2)$$

where C_i denotes the activity of species i in the sediment (decays/s); D_s is the molecular diffusion coefficient of species i in the sediment (cm^2/s); D_r is the radial diffusion coefficient of solute i in sediments (cm^2/s); x is depth from the sediment–water interface (cm, positive down); r ($r_1 \leq r \leq r_2$) is the distance from the axis of the hollow burrow cylinder (cm); r_1 and r_2 are the radii of the hollow burrow cylinder and the

average microenvironment, respectively (cm); λ is the radioactive decay rate (s^{-1}); and t is time (s). Aller (24) solved this model for steady-state conditions ($\partial C_i / \partial t = 0$), but in this study the transient case (eq 2) is solved. In the lower undisturbed zone, there are no burrows so that solute transport can be described simply as vertical molecular diffusion with radioactive decay. The boundary conditions for the system are (1) the concentration at the sediment–water interface is equal to the constant value of the overlying water column; (2) the gradient at the bottom of the mixed layer is equal to the gradient at the top of the buried sediment; (3) the concentration at the inside of the burrow wall is equal to the concentration in the overlying water column; and (4) the concentration gradient at the outside margin of the microenvironment is equal to zero.

The major parameters in the cylindrical model include D_s , D_r , L , r_1 , and r_2 . r_1 , r_2 , and L can be directly measured from the burrows. D_s can be determined from the control cell as described above in the enhanced diffusion model. The rate of diffusion of solutes across burrow walls, D_r , depends on the permeability of burrow lining materials, the permeability and thickness of the burrow wall, sediment porosity near the burrow wall, chemical reactions affecting sediment properties near the burrow wall, the biogenic irrigation rate, and microbial activity (41). In this study, it is assumed that D_r is equal to D_s .

Nonlocal Solute Exchange Model. Emerson *et al.* (27) proposed a simple, one-dimensional diffusion model with an additional source or sink term, α , which accounts for any mode of transport between nonadjacent points in the sediment or between the overlying water and points in the sediment removed from the sediment–water interface. The model has been coined the “nonlocal exchange model” (28) and has been widely used (30, 34–38, 42) in other solute transport studies. The advantages of the model are that there is no need to determine the average micro-environment parameters as in the cylindrical burrow model; that it can be used to quantify the exchange by any bioturbation mechanism without the need to describe the mechanism if α can be properly described and that it is easy to solve model equations. The disadvantage is that it requires determination of the term α , which is to a large extent empirical. In many cases, α varies for different solutes and animal species as well as with depth and time. Boudreau (1) proved the equivalence of the nonlocal exchange model and the cylindrical burrow model under certain assumptions, but he concluded that not all nonlocal exchange models were equivalent to the cylindrical burrow model, because a large class of transport phenomena that could be described by nonlocal exchange models cannot be represented by the cylindrical burrow model. In the mixed zone, pore water and solute transport can be categorized as one of these processes: (1) random diffusion across the sediment–water interface; (2) exchange between discrete points in the sediment or between the overlying water and the pore water in the sediment due to biological irrigation or pumping of burrows; and (3) advection caused by sedimentation. Solute concentrations also may be affected by reactions such as oxidation–reduction, precipitation, and radioactive decay. Because there is no external sedimentation in these laboratory experiments, sediment burial can be ignored. Solute transport in the mixing zone can be described as

$$\frac{\partial C_i}{\partial t} = D_s \frac{\partial^2 C_i}{\partial x^2} - \alpha(C_i - C_0) - \lambda C_i \quad (3)$$

where C_i is the activity of solute i in bulk sediment (decays/s); C_0 is the activity of solute i at the sediment–water interface (decays/s); D_s is the molecular diffusion coefficient of solute in bulk sediment corrected for sediment tortuosity and porosity and assumed constant with depth (cm^2/s); α denotes

the fraction of nonlocal exchange per unit time (s^{-1}); x is the depth from the sediment–water interface (cm, positive down); λ is the radioactive decay constant (s^{-1}); and t is time (s). The first term on the right-hand side of the equation accounts for molecular diffusion of solutes in sediments; the second term accounts for nonlocal biogenic exchange of solute; and the third term accounts for the changes caused by radioactive decay of the tracer. Below the mixed layer, there is no biological nonlocal exchange of solutes; therefore, $\alpha = 0$. The boundary conditions include (1) the concentration at the sediment–water interface is equal to the constant value of the overlying water column; (2) the gradient at the bottom of the mixed layer is equal to the gradient at the top of the buried sediment; (3) the concentration gradient at depth in the sediment column is equal to zero. Two transport parameters need to be evaluated in the model: D_s and α . The procedure for the evaluation of D_s is exactly the same as in the other models, that is, to evaluate D_s from the transport profiles of control cells. However, there is no established method for the evaluation of α simply because the depth dependency of α and the relations between α and transport mechanisms and burrow lining properties are still unclear. Several studies have found values for α in the range of 1×10^{-7} – $2 \times 10^{-6} \text{ s}^{-1}$ (27, 32, 33, 36, 42). In each of the laboratory experiments of this study, only a single species and size of animal was used. It is reasonable to assume that α does not vary dramatically within the bioturbated layer in our experiments. α was estimated for each microcosm by substituting different values of α into the nonlocal exchange model and comparing the results with the measured tracer activity profiles to find a best fit.

Discussion

The mechanisms of solute transport by *Branchiura sowerbyi* can be evaluated by examining differences between measured profiles and modeled results. In this way, not only will the best values of model parameters for *B. sowerbyi* be determined but also the advantages and disadvantages of each model will be demonstrated. The ^{22}Na activity profiles of *B. sowerbyi* shown in Figures 2–4 exhibited apparent enhanced diffusion. The ^{22}Na diffusion rate increases with increasing population density. Therefore, there is reason to assume that solute transport across the sediment–water interface by the activities of burrowing deposit-feeding *B. sowerbyi* worms is basically a diffusive process and the transient enhanced diffusion model should be able to describe the transport process closely. Model fits of the downward migrating diffusion front are shown in Figure 2 for the control cell, Figure 3 for the cell with 2 *B. sowerbyi* worms, and Figure 4 for the cell with 4 *B. sowerbyi* worms. The mixing depths are greater than the 10 cm shown in Figures 2–4, but the model simulates the entire length of the sediment column (~ 23 cm).

In the cell with 4 *B. sowerbyi* worms, the rate of diffusion of ^{22}Na was a little lower at the beginning of the experiment and started to increase rapidly after about 4 days, probably because of the animal acclimatization period. Both cells with organisms yielded much higher diffusion coefficients than the control cell ($D_s = 49.17 \pm 4.09 \text{ cm}^2/\text{yr}$). The values of D_e from the cells with 2 worms ($D_e = 91.69 \pm 3.76 \text{ cm}^2/\text{yr}$) and 4 worms ($D_e = 234.9 \pm 19.7 \text{ cm}^2/\text{yr}$) are 1.87 and 4.78 times the value of the D_s in the control, respectively. This means that *B. sowerbyi*, which is a very important sediment particle transporter, is also very important in solute transport across the sediment–water interface. Furthermore, the influence of population density on D_e is significant. As the population density is doubled, D_e increased by a factor of 2.6. This cannot be attributed to a difference in porosities, because the cell with 2 *B. sowerbyi* had a higher porosity than the cell with 4 *B. sowerbyi*. Apparently an increase in the numbers of organisms greatly increases burrowing and deposit-feeding activities, which enhances both the particle and solute

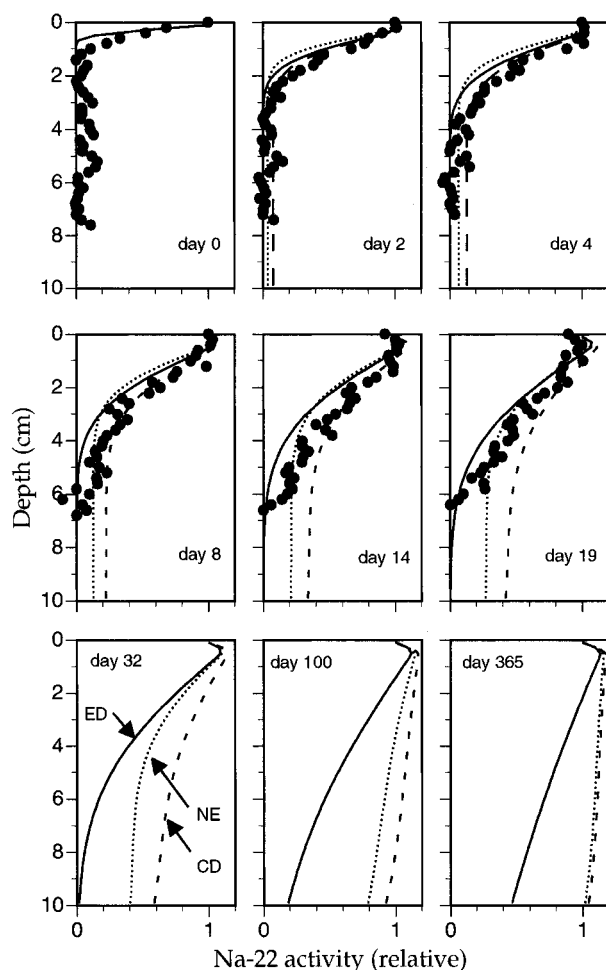


FIGURE 5. Model simulation results of the ^{22}Na activity in the cell containing 2 *B. sowerbyi* worms (~ 4000 individuals/ m^2). ED and solid line, enhanced diffusion model (eq 1); CD and dashed line, cylindrical diffusion model (eq 2); NE and dotted line, nonlocal exchange model (eq 3).

transport rates. Such mixing and feeding increased the communication between the overlying water and the pore fluid and between pore fluids at different depth intervals and thus greatly enhanced the apparent diffusivities of solutes in sediments.

The values of D_e obtained from modeling the downward migrating diffusion front were substituted into the enhanced diffusion model (eq 1) to simulate the ^{22}Na profiles in the cells containing *B. sowerbyi* worms. The simulation results

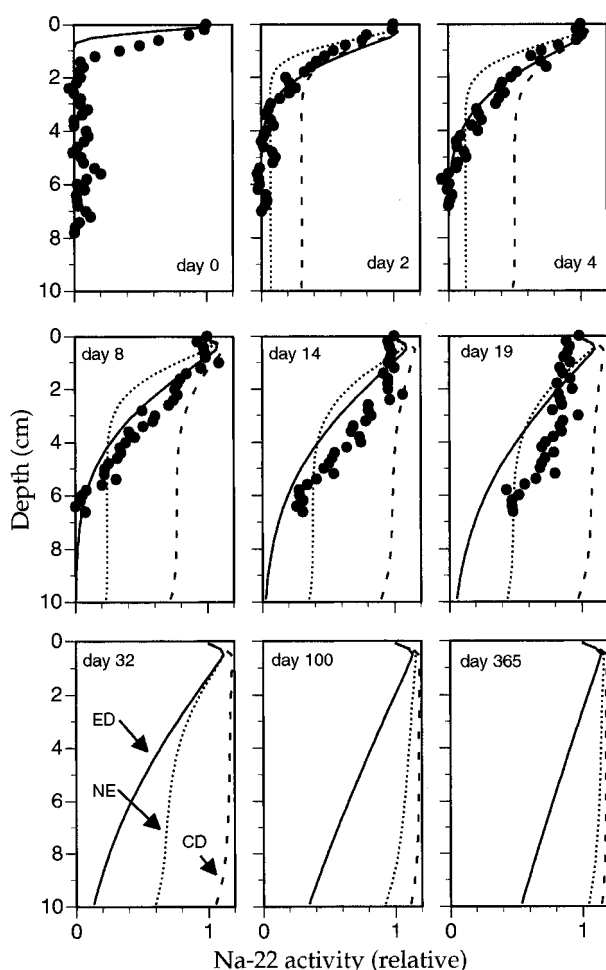


FIGURE 6. Model simulation results of the ^{22}Na activity in the cell containing 4 *B. sowerbyi* worms (~ 8000 individuals/ m^2). ED and solid line, enhanced diffusion model (eq 1); CD and dashed line, cylindrical diffusion model (eq 2); NE and dotted line, nonlocal exchange model (eq 3).

are shown in Figures 5 and 6 along with the experimental data and the results from the other models (see below). The parameters used in the model simulations are listed in Table 1. The drop of ^{22}Na activity near the sediment–water interface is due to an optical effect of the detector collimator because the cells only had a ~ 6 cm overlying ^{22}Na -spiked water column. The model describes reasonably well the values and general shapes of the profiles, indicating that solute transport in the presence of *B. sowerbyi* worms is primarily by enhanced

TABLE 1. Model Simulation Parameters Used To Generate Curves in Figures 5 and 6

parameter	2000 <i>B. sowerbyi</i> / m^2	4000 <i>B. sowerbyi</i> / m^2	description
λ (yr)	2.6	2.6	tracer half-life
C_0	1	1	tracer activity at surface
bkg	0	0	background activity
D_e (cm^2/yr)	91.69	234.9	enhanced biodiffusion coefficient
D_s (cm^2/yr)	49.17	49.17	molecular diffusion coefficient
D_r (cm^2/yr)	49.17	49.17	radial diffusion coefficient
r_1 (cm)	0.1	0.1	average burrow radius
r_2 (cm)	2.5	1.25	average microenvironment radius
dr (cm)	0.1	0.1	radial simulation interval
α (1/yr)	5	10	nonlocal exchange coefficient
L (cm)	13.62	11.74	thickness of mixing layer
T_x (cm)	23	23	total simulated depth
dx (cm)	0.2	0.2	simulation depth interval
T_t (day)	365	365	total simulated time
dt (day)	0.025	0.025	simulation time step
σ (cm)	0.22	0.22	detector efficiency

diffusion. On day 19 in the cell with 2 worms, the model slightly overestimates the ^{22}Na activities in the top 1 cm. Below 1 cm, the model systematically underestimates the activities. This is especially apparent in the cell with 4 worms, where at between 2 and 5 cm, the measured data are significantly higher after 8 days. The difference becomes greater with increasing time. This is because the model does not account for rapid direct exchange caused by burrowing activities. In the experiment, it was observed that the worms built a very complicated dense burrow system. When the organisms burrowed from the surface into the substratum, some overlying water containing ^{22}Na was incorporated into the sediment. This input cannot be described as a diffusional process and is dependent on the burrow depth, burrow density, and connection between the burrow and the overlying water column. Because the worms usually destroyed old burrows when building new ones and did not ventilate the burrows with the overlying water-like suspension filter feeders, this rapid direct exchange was normally not very important. However, if the burrows are not destroyed and are open at the top for communication with the overlying water, they can act as conduits for direct solute exchange between the overlying water and the pore fluid. Because the population density is doubled in the cell with 4 worms, the burrowing activities were more intense, and therefore the rapid direct exchange was greater. In addition, sediment recycling due to the conveyor-belt feeding of the worms also resulted in significant downward migration of surficial sediments that caused vertical advection of ^{22}Na into the sediment. This effect is not considered in the model. The model simulation was continued for 1 yr, and the total activity (mass) of ^{22}Na that accumulated in the sediment was calculated to be 9.06 times the ^{22}Na mass in the overlying water during the experiment in the cell with 2 *B. sowerbyi* and 10.04 times that of the overlying water in the cell with 4 worms.

The cylindrical diffusion model (eq 2) was also applied to the two cells containing *B. sowerbyi* worms for the purpose of comparing different solute transport mechanisms. The parameters used in the model calculations are listed in Table 1. In Figures 5 and 6, it can be seen that the cylindrical diffusion model simulates the ^{22}Na activity in the cell with 2 worms fairly well in the first 8 days, but overestimates the downward transport after that. The deviation becomes greater at depth. This overestimation effect is more pronounced in the cell with 4 *B. sowerbyi* worms where the simulated ^{22}Na activity is consistently higher than the measured data at all times and at all depths. This suggests that the burrows of *B. sowerbyi* were not irrigated with the overlying water, at least not for the full length. Any enhanced solute transport due to the presence of burrows is significantly less than that calculated assuming the burrows are irrigated with overlying water. Therefore, solute transport by *B. sowerbyi*, even though it is important, cannot be adequately described as an irrigated cylindrical diffusional process.

Figures 5 and 6 also show the results of the nonlocal exchange model simulations. Model values for α and other parameters are given in Table 1. The values obtained for α ($1.6\text{--}3.2 \times 10^{-7} \text{ s}^{-1}$) are in agreement with those obtained by Emerson *et al.* (27) and by Hammond *et al.* (32) from Puget Sound sediment ($1\text{--}5 \times 10^{-7} \text{ s}^{-1}$). It can be seen that the model gives fairly good predictions of the ^{22}Na activity except that there is a little underestimation in the top 1–5 cm and some overestimation below 6 cm. Since a constant α was used for the mixed layer, an increase or decrease in α would only proportionally increase or decrease the simulated activity throughout the entire mixed layer. So, it is not possible to account for the underestimation in the upper zone and the overestimation in the lower zone simply by varying the value of α . It is possible that α might have a higher value in the upper zone and a lower value in the lower zone. Martin and Sayles (42) and Martin and Banta (36) adopted a depth-

dependent form for α in which α exhibited a maximum at the sediment–water interface and an exponential decrease with depth. In this study, however, the benthic population was restricted to a few organisms of similar size in homogeneous sediment, so a constant value of α is more reasonable than a nonlocal exchange coefficient that decreases with depth. The poor fit indicates that either the transport is depth dependent or there are other transport processes that cannot be accounted for by a single nonlocal exchange coefficient. The simulations were continued for 1 yr, and the calculated ^{22}Na mass that accumulated in the sediment was 16.45 and 16.20 times the ^{22}Na activity (mass) in the overlying water during the experiment for the cells with 2 *B. sowerbyi* and 4 *B. sowerbyi*, respectively. Since the nonlocal exchange model and the cylindrical diffusion model are equivalent under some conditions (1), it might be expected that the two models should yield identical results. The models do produce activity profiles that exhibit similar behaviors in both depth and time. However, they do not yield precisely the same results, especially in the transient model case, because the burrow geometries were measured in the cylindrical burrow model and the exchange coefficient was a model fit parameter in the nonlocal model case. In addition, the exchange model can account for nonlocal exchange processes that are not described by the irrigated burrow model, such as downward transport of solute by particle mixing.

The oligochaete *B. sowerbyi*, is the largest conveyor-belt feeding freshwater worm and the only freshwater annelid to even approach the size of marine worms. *B. sowerbyi* also has a widespread distribution, but it has been little studied. Soster (11) reported densities ranging from 0–584/m² for *B. sowerbyi* in Lake Erie, and Kikuchi and Kurihara (10) reported a population density of 8842/m² for *B. sowerbyi* in ricefield soils in Japan. These natural densities are similar to those used in the experiments, so the effects reported here for enhanced solute transport by *B. sowerbyi* would be expected to be similar to those actually occurring in natural settings. The Great Lakes are currently undergoing radical shifts in benthos distribution and abundance patterns because of the recent invasion of *Dreissenid* bivalves (zebra mussels). Zebra mussels are modifying the nutrient and carbon flow in the ecosystem in ways that we do not yet understand. The results of this study demonstrate that *B. sowerbyi* has a significant impact on solute transport in muddy sediments and that this impact is density dependent. As we begin to assess the long-term impact of the mussels on the Great Lakes, the importance of large infauna, such as *B. sowerbyi*, on the biogeochemical cycling of nutrients and other chemical species needs to be considered.

Acknowledgments

Peter McCall assisted in the collection of sediment and test animals and in the operation of the γ -scanner. This work was supported by EPA Contract R-817278-01-0.

Literature Cited

- (1) Boudreau, B. P. *J. Mar. Res.* **1984**, *42*, 731–735.
- (2) Aller, R. C. In *Animal-Sediment Relations: The Biogenic Alteration of Sediments*; McCall, P. L., Tevesz, M. J. S., Eds.; Plenum: New York, 1982; pp 53–102.
- (3) Fisher, J. B. In *Animal-Sediment Relations: The Biogenic Alteration of Sediments*; McCall, P. L., Tevesz, M. J. S., Eds.; Plenum: New York, 1982; pp 177–218.
- (4) Matisoff, G.; Fisher, J. B.; Matis, S. *Hydrobiologia* **1985**, *122*, 19–33.
- (5) Rhoads, D. C. *Oceanogr. Mar. Biol. Annu. Rev.* **1974**, *12*, 263–300.
- (6) Robbins, J. A.; McCall, P. L.; Fisher, J. B.; Krezoski, J. R. *Earth Planet. Sci. Lett.* **1979**, *42*, 277–287.

- (7) Krezoski, J. R.; Robbins, J. A. *J. Geophys. Res.* **1985**, *90* (C6), 11999–12006.
- (8) McCall, P. L.; Fisher, J. B. In *Aquatic Oligochaete Biology*; Brinkhurst, R. O., Cook, D. G., Eds.; Plenum: New York, 1980; pp 253–317.
- (9) Krezoski, J. R.; Robbins, J. A.; White, D. S. *J. Geophys. Res.* **1984**, *89* (B90), 7937–7947.
- (10) Kikuchi, E.; Kurihara, Y. *Oikos* **1977**, *29*, 348–356.
- (11) Soster, F. M. Ph.D. Dissertation, Case Western Reserve University, 1984.
- (12) Appleby, A. G.; Brinkhurst, R. O. *J. Fish. Res. Board Can.* **1970**, *27*, 1971–1982.
- (13) Wang, X. Ph.D. Dissertation, Case Western Reserve University, 1995.
- (14) Schink, D. R.; Guinasso, N. L., Jr.; Fanning, K. A. *J. Geophys. Res.* **1975**, *80*, 3013–3031.
- (15) Schink, D. R.; Guinasso, N. L., Jr. *Mar. Geol.* **1977**, *23*, 133–154.
- (16) Schink, D. R.; Guinasso, N. L. *Am. J. Sci.* **1978**, *278*, 687–702.
- (17) Goldhaber, M. B.; Aller, R. C.; Cochran, J. K.; Rosenfeld, J. K.; Martens, C. S.; Berner, R. A. *Am. J. Sci.* **1977**, *277*, 193–237.
- (18) Vanderborght, J. P.; Wollast, R.; Billen, G. *Limnol. Oceanogr.* **1977**, *22*, 787–793.
- (19) Aller, R. C. *Am. J. Sci.* **1978**, *278*, 1185–1234.
- (20) Cochran, J. K. *Earth Planet. Sci. Lett.* **1980**, *49*, 381–392.
- (21) Matisoff, G. In *Animal-Sediment Relations: The Biogenic Alteration of Sediments*; McCall, P. L., Tevesz, M. J. S., Eds.; Plenum: New York, 1982; pp 289–330.
- (22) Hammond, D. E.; Simpson, H. J.; Mathieu, G. In *Marine Chemistry in the Coastal Environment*; Church, T. M., Ed.; American Chemical Society Symposium Series 18; American Chemical Society: Washington, DC, 1975; pp 119–132.
- (23) Aller, R. C. Ph.D. Dissertation, Yale University, 1977.
- (24) Aller, R. C. *Geochem. Cosmochim. Acta* **1980**, *44*, 1955–1965.
- (25) Aller, R. C. In *Advances in Geophysics, Volume 22*; Saltzman, B., Ed.; Academic Press: New York, 1980; pp 237–350.
- (26) Wang, X.; Matisoff, G. To be submitted to *Limnol. Oceanogr.*
- (27) Emerson, S.; Jahnke, R.; Heggie, D. *J. Mar. Res.* **1984**, *42*, 709–730.
- (28) Imboden, D. M. Habilitation Thesis, Swiss Federal Institute of Technology, 1981.
- (29) Christensen, J. P.; Devol, A. H.; Smethie, W. M. *Cont. Shelf Res.* **1984**, *3*, 9–23.
- (30) Christensen, J. P.; Murray, J. W.; Devol, A. H.; Codispoti, L. A. *Global Biogeochem. Cycles* **1987**, *1*, 97–116.
- (31) Hammond, D. E.; Fuller, C. In *San Francisco Bay: The Urbanized Estuary*; Comomos, T. J., Ed.; American Association for the Advancement of Science: San Francisco, 1979; pp 213–230.
- (32) Hammond, D. E.; Fuller, C.; Harmon, D.; Hartman, B.; Korosec, M.; Miller, L. G.; Rea, R.; Warren, S.; Berelson, W.; Hager, S. W. *Hydrobiologia* **1985**, *129*, 69–90.
- (33) Aller, R. C.; Yingst, J. Y. *J. Mar. Res.* **1985**, *43*, 615–645.
- (34) Viel, M.; Barbanti, A.; Langgone, L.; Buffoni, G.; Paltrinieri, D.; Rosso, G. *Estuarine, Coastal Shelf Sci.* **1991**, *33*, 361–382.
- (35) Archer, D.; Devol, A. *Limnol. Oceanogr.* **1992**, *37*, 614–629.
- (36) Martin, W. R.; Banta, G. T. *J. Mar. Res.* **1992**, *50*, 125–154.
- (37) Devol, A. H.; Christensen, J. P. *J. Mar. Res.* **1993**, *51*, 345–372.
- (38) Marinelli, R. L. *Limnol. Oceanogr.* **1994**, *39* (2), 303–317.
- (39) Berner, R. A. *Early diagenesis: A theoretical approach*; Princeton University Press: New York, 1980.
- (40) Matisoff, G. In *Metal Contaminated Aquatic Sediments*; Allen, H. E., Ed.; Ann Arbor Press: Chelsea, MI, 1995; pp 201–272.
- (41) Aller, R. C. *J. Mar. Res.* **1983**, *41*, 299–322.
- (42) Martin, W. R.; Sayles, F. L. *Geochem. Cosmochim. Acta* **1987**, *51*, 927–943.

Received for review August 19, 1996. Revised manuscript received March 3, 1997. Accepted March 5, 1997.*

ES960716N

* Abstract published in *Advance ACS Abstracts*, May 1, 1997.